Wideband, High Gain, High Linearity, Low Noise Amplifier for GNSS Frequencies with Compensation for Low Frequency Instability

Sarang Thombre, Heikki Hurskainen, Jari Nurmi
Department of Computer Systems
Tampere University of Technology (TUT)
Tampere, Finland
{sarang.thombre, heikki.hurskainen, jari.nurmi}@tut.fi

Abstract— **This paper presents the design methodology, simulation results and implementation details of a low noise amplifier (LNA) designed to operate over the whole range of Global Navigation Satellite System (GNSS) frequencies (1164MHz to 1615.5MHz). This LNA works over combined (but overlapping) frequency bands of all three GNSS constellations (GNSS consist of the American Global Positioning System (GPS), European Galileo system and the Russian GLONASS system). Designed to be unconditionally stable with gain of over 18dB and noise figure of 2dB over a considerable bandwidth of about 450MHz, the achieved results conformed quite well to the specifications. Final implementation results include a gain of 18.5dB at the centre frequency with a nominal variation of ±1.3dB over the desired bandwidth. The noise figure obtained is 2.18dB and the amplifier stability range extends from 0Hz to 9GHz. Very high degree of linearity is achieved with output 1dB compression at +13dBm and output third order intercept at +23dBm. This paper describes results at every stage of design, simulation and implementation along with a solution against typical low frequency instability by a small trade-off in noise figure.**

Keywords-wideband, high gain, high linearity, GNSS, LNA, amplifier, stability, RF, low frequency instability

I. INTRODUCTION

Most of the current GNSS receiver radio frequency (RF) front-ends are tuned for L1 band (centered at 1575.42MHz) reception, since it is one of the frequencies used by GPS. In future, the RF front-ends need to be more versatile and capable of receiving wider range of frequencies due to introduction of new satellite navigation systems, e.g. Galileo which transmits signals at E1 (centered at 1575.42 MHz), E5 (centered at 1191.795MHz) and E6 (centered at 1278.75MHz) [1]. Modernized GPS will add civilian signal to L2 (centered at 1227.6MHz) and L5 (centered at 1176.45MHz) [2] and GLONASS system is using frequencies of L1 (centered at 1602MHz) and L2 (centered at 1246MHz) [3].

For some years there has been considerable interest in the bandpass sampling based RF front-end design. In [4], bandpass sampling of a single band of frequencies was considered which evolved to sampling multiple distinct RF bands in [5], [6] and [7]. In [8], bandpass sampling of multiple distinct single-sided (complex) RF bands was accomplished. In all these works, either GPS and GLONASS or GPS and GSM signals were integrated and that too, just L1 band signals in each case. [9] claims to use bandpass sampling and digital filtering for direct conversion of GPS L1 (C/A) and L1/L2 (P(y)) codes into digital intermediate frequency (IF).

The RF front-end architecture presented in Figure 1 is built around the concept of bandpass sampling of the entire GNSS frequency spectrum using a wideband LNA, filters and an analog to digital converter (ADC) and then performing the channel selection in the digital domain using digital filters and multi-rate signal processing. As the first step towards full implementation of this front-end architecture, the LNA was designed, simulated and implemented as a stand-alone circuit on printed circuit board (PCB). This paper details the results for this LNA.

Some research has already been performed towards designing LNAs working on or around the frequency range of interest. For example, in [10] a 65nm CMOS LNA for multi-standard radio applications between 100MHz and 6GHz is described. Its strengths are its wide bandwidth, low silicon area ($0.01mm^2$) and low power consumption (21mW). On the other hand, its gain and noise figure are 15dB and 3dB respectively. In [11], an LNA for GNSS frequencies is described. It is a PCB based design with a gain of 16.7dB. Similarly, in [12] a wideband LNA for GNSS frequencies is constructed. Here also, the LNA is a PCB based implementation with a gain of 15.5dB and power consumption of 2.2W.

Figure 2 shows the GNSS frequency spectrum on which the front-end and the LNA is designed to operate. The LNA is required to amplify a bandwidth of 451.5 MHz (1164MHz to 1615.5MHz). Power gain over this bandwidth should be atleast 18dB with a maximum deviation of ±1.5dB. Maximum noise figure should be 2dB and the minimum requirement for 50Ω impedance matching is that return loss at input and output

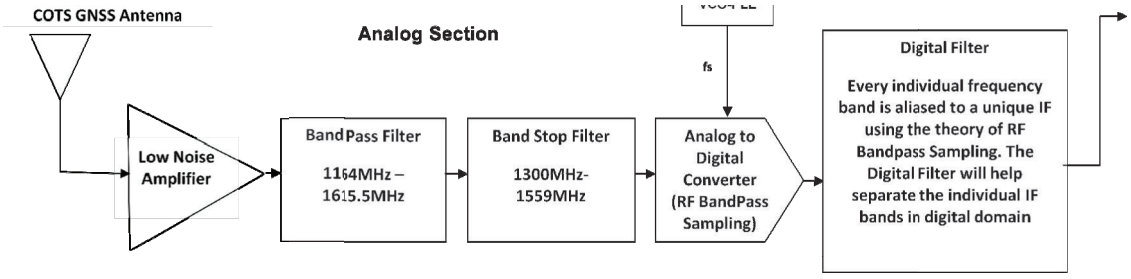

Figure 1. Block diagram of a bandpass sampling RF front-end for GNSS Receivers

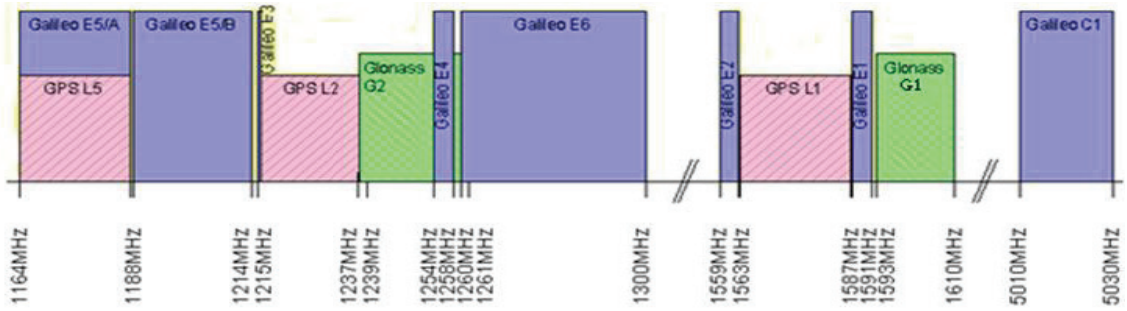

Figure 2. Future GNSS frequency spectrum [13]

should be less than -10dB. It should also be inherently stable over all frequencies, while output one-dB compression should be atleast +3dBm. A decision was made on using the BFP420 transistor from Infineon [14] because its gain and noise figure ratings were in conformance with the desired specifications. All simulations have been performed in Agilent ADS simulation software.

The outline of the paper is as follows. Section II describes the design of the support circuitry for the LNA. This includes the biasing, stabilization and input and output impedance matching circuits. Section III describes the simulation stage where the entire LNA circuit (including support structures and transmission line effects) were simulated using Agilent ADS software. Section IV describes the issue of and solution against low frequency instability typical to amplifiers that are impedance matched for high gain. The final implementation and PCB layout are described in Section V. The LNA structure was finalized only after many candidate structures were simulated and their limitations analyzed. These structures and their shortcomings are also described in this section. Section VI shows the results of the final implementation. It shows that this LNA is indeed wideband, high gain, highly linear, low noise and inherently stable over the GNSS frequency range.

II. Design Stage

The biasing network is responsible for setting the correct DC operating voltage and current for the transistor within an LNA circuit. The supply voltage and current was standardized at 5 volts and 20mA DC respectively. With proper design of biasing resistors, the desired operating voltage and current were achieved. An important point to note is the role of the emitter inductance. When the emitter of the amplifier is connected to ground via a hole in the PCB, this adds a certain inductance (usually assumed to be less than 1nH). It was found that this inductance lowers the gain of the amplifier by about 1-3dB and is unavoidable. Hence it should always accompany the transistor model in simulations.

The LNA is specified to be unconditionally stable from 0Hz to f_{max}. Here f_{max} is equal to the maximum frequency of oscillation of our transistor, BFP420, which is 25GHz. Since the S-parameter file for BFP420 had empirical data between 100MHz and 9GHz, it was possible to test the stability only within this frequency range. It is safe to assume that if the LNA is stable up to 9GHz, at higher frequencies the losses of the components and transmission line segments are so high that the reduced gain most probably negates any possibility of instability. Before a stabilization circuit was designed, the LNA was unstable after 3GHz. Therefore, a sub-circuit was designed that would take care of high frequency gain. One idea was to add a series resistance in the output circuit and tune all component values again to achieve best gain, noise figure and unconditional stability.

The amplifier should be impedance matched perfectly to 50 ohms at input and output. However, there are usually two methods by which impedance matching can be done, each with its unique advantage [15], [16]. It is possible to either match for maximum gain, using technique of simultaneous conjugate matching, or minimum noise figure using noise and available gain circles. It is even possible to match the input for minimum noise figure and output for maximum gain. It was decided to match the LNA for maximum gain using the principle of simultaneous conjugate matching. 'Matched' source (Γ_{ms}) and load (Γ_{ml}) reflection coefficients were plotted on Smith-Chart. Next, their value at the centre frequency was found and an appropriate LC matching network was designed using RFDude software [17] to match 50Ω input and output terminations to complex conjugates of these reflection

coefficients. Once the passive matching components are derived, they are inserted in the correct order starting from source and load impedances. Then the components are again tuned for best gain, noise figure and stability.

III. Simulation Stage

All the constituent blocks of the LNA were individually simulated and all the passive components were tuned to achieve perfect DC biasing conditions and maximum gain yet keeping all other parameters as close as possible to the specifications. The schematic was then re-simulated by considering all possible effects that may degrade the performance. There is one important effect that has to be taken into consideration - effect of transmission line (TL) segments in the RF path. When RF signals pass through the copper conductor, the conductor acts as a lossy TL and its effects have to be taken into account. TL effects are directly proportional to the physical dimensions of the TL segment. In the schematic of ADS, all copper conductors in the RF path were replaced with TL segments of length and width equal to that of the actual conductor. The width and length information can be obtained from the layout by placing a RULER component from the ADS Layout Tool at any conductor that is to be measured. The passive components were once again tuned for maximum gain.

Even though it is not possible to model all parasitic and TL effects perfectly, inclusion of the TL segments brings the simulation model very close to real world scenario. Figures 3, 4, 5, and 6 show final simulation results after designing all support circuitry and taking into account TL effects. Figure 3 shows the gain (given by S parameter S_{22}) of LNA versus frequency plot. At the desired center frequency, gain is 17.15 dB and very close to our specification of 18dB. This difference of 1dB between the desired and simulated gains was compensated for in the actual implementation as shown in Section V of this paper. Figure 4 shows the input reflection co-efficient (S_{11}) versus frequency plot. It shows that perfect 50Ω matching at input is achieved over the entire desired bandwidth since S_{11} is less than -10dB in this region. Similarly, Figure 5 shows the output reflection coefficient (S_{22}) versus frequency plot. Here near-perfect output matching is also achieved over the entire desired bandwidth.

Figure 6 shows the noise figure of the simulated LNA. The curve nf(2), shows the actual noise figure and it is very close to our desired value of 2dB over the entire bandwidth. An interesting observation is that the gain falls drastically around 3.75GHz. Consequently, the noise figure is extremely high in the same frequency region. The reason can be found from figures 4 and 5 which show poor input and output impedance matching at the same frequency. This is most probably the consequence of TL effects considered in the final simulations. However, since 3.75GHz is very far from the GNSS band, we can safely ignore this phenomenon.

IV. Low Frequency Instability Issue

During the actual implementation, it was observed that the LNA was unstable at frequencies below 1GHz. The 'μ' stability factor derived for the source and load ends of the LNA has to be greater than unity over all frequencies for the LNA to be stable. However, as shown in Figure 7, the value of 'μ' goes

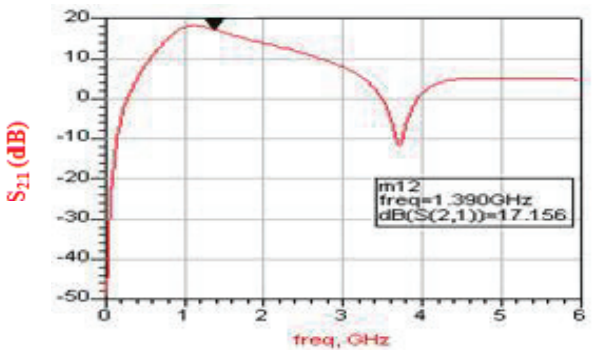

Figure 3. Gain VS Frequency after transmission line effects.

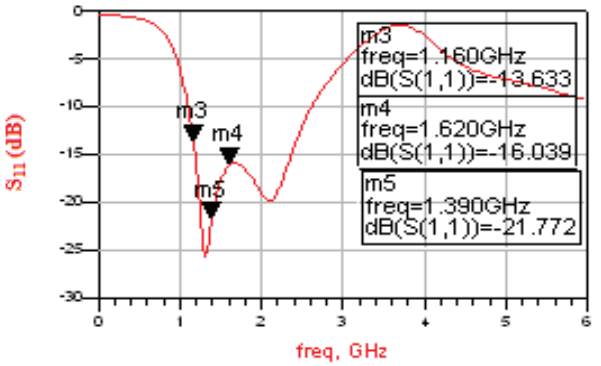

Figure 4. Input return loss curve after transmission line effects

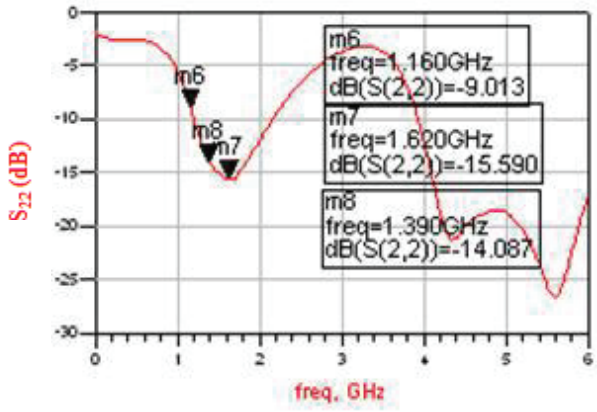

Figure 5. Output return loss after transmission line effects

below unity at around 1GHz. This instability issue was successfully solved by a slight compromise on the noise figure of the LNA.

Two possible solutions to this instability:

1. Parallel resonant circuit centered at about 500MHz.
2. Resistor stabilization.

Both options basically aim to lower the gain at low frequencies to remove the instability. They were prototyped one after the other. After implementing the resonant circuit the noise figure remained unchanged and the LNA became stable at low frequencies as expected. However, this also resulted in the input and output matching being disturbed and consequently, a reduced overall gain (16.5dB).

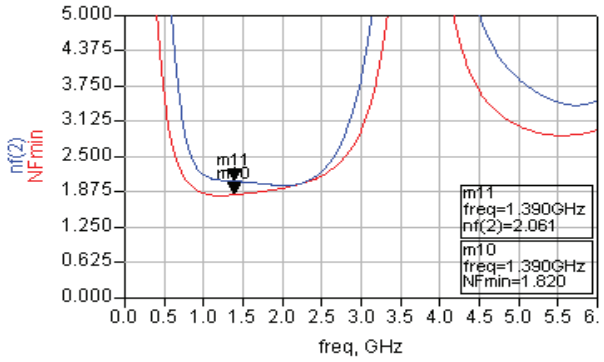

Figure 6. Noise figure VS frequency

Figure 7. Plot of the 'μ' stability factor showing instability at low frequencies

In resistor stabilization, possible configurations are: a series resistor in input or output, parallel resistor in input or output and a combination of both in input or output. The parallel resistors disturb the matching quite a lot while resistors in the output had a limited effect on the matching. Hence, it was decided to use a single resistor in series in the input of the transistor. When the series resistor of 4.3Ω was used, the amplifier became stable at low frequencies, the gain reduced, but was still over the specified 18dB and the input and output matching improved. However, the series resistor added noise and the overall noise figure increased slightly to 2.18dB. Table 1 shows the various stabilization schemes tested and their results.

V. Final Implementation

Before the final implementation version could be reached, the LNA had to go through some initial test versions, each with its limitations that were identified and resolved in the subsequent versions. Version 1 had a gain of 8dB and noise figure in excess of 2.2dB. At this stage it was realized that taking into consideration TL effects in software simulation is necessary to design correct values of impedance matching elements. For version 2 of the LNA, new values of matching and stabilization elements were designed and consequently the gain nearly doubled to 15dB while noise figure dropped to 1.8dB. In spite of the encouraging results, it was observed that the impedance matching was not yet perfect as the input and output return loss was not below -10dB over the bandwidth. Therefore, in version 3 efforts were made to perfect the impedance matching sub-circuits. As a result, the gain increased to 19.2dB and noise figure further improved to 1.72dB. However, now the LNA was unstable at frequencies slightly below 1GHz due to the increased gain. Version 4 (final

TABLE 1. Various stabilization schemes attempted

Possible solution	Input or Output	Outcome	OK?
Series resonant circuit	Input	➢ Stability achieved, NF maintained ➢ Matching disturbed ➢ Gain degrades	No
Series resistor	Output	➢ Stability not achieved ➢ OIP3, P1dB disturbed ➢ NF, gain, matching maintained	No
Parallel resistor	Output	➢ Stability not achieved ➢ Matching disturbed	No
Parallel resistor	Input	➢ Stability not achieved ➢ Matching disturbed	No
Capacitor between VCC & ground	DC biasing circuitry	➢ Instability improved but not completely removed	No
Series resistor	Input	➢ Stability achieved ➢ Matching maintained ➢ NF disturbed	Yes

version) utilized the series resistor solution to improve stability as explained in section IV of this paper. At this point, the LNA had satisfied all design requirements.

The schematic of the final version of the LNA is shown in Figure 8. Resistors R2 and R1 are the biasing resistors while capacitor C1 is for grounding any RF energy that may enter the DC biasing circuit. Inductors L3 and L7 are RF chokes which also block any RF energy from entering the 'DC area' of the circuit. Resistor R3 is the series resistor added to compensate for low frequency instability as explained in section IV. Capacitor C3 is the output DC blocking capacitor. It does not allow DC energy to flow in the RF signal path in the direction of output. Capacitor C5 has a dual role – DC blocking and input impedance matching. Parallel combination of C6 and L6 form the output matching sub-circuit. Inductor L1 simulates the parasitic inductance of the hole in the PCB through which emitter pin of the transistor is grounded (explained in section II). Z_{in} and Z_{out} are dummy 50Ω source and load impedances respectively.

Figure 9 shows the layout of the final version to be etched on PCB. The RULERs are added to show the actual size of the final circuit PCB which is 5.5cm x 2.5cm. The LNA was created from an academic view point as a proof of concept for the bandpass sampling radio front-end and hence, only moderate effort was put into utilizing minimum area or integration on silicon. Similarly, minimization of power consumption was also not a critical requirement at present. We plan to design all individual blocks of the bandpass sampling RF front-end as stand-alone circuits on PCB and once the front-end is operational, future studies with more strenuous power consumption limits may follow.

VI. Results

Results for the final implementation of the low noise amplifier are shown in Figures 10 to 13 and they show that the implementation of the design was successful not only at the centre frequency but also over the entire bandwidth of interest. The LNA centre frequency was 1389.75MHz (The desired band was from 1164MHz to 1615.5MHz) and the gain at this centre frequency is marked in Figure 10 by the s-parameter

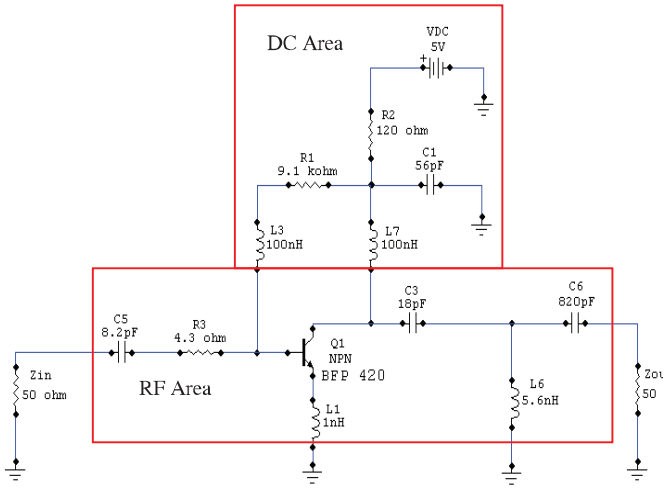

Figure 8. Simplified schematic of the final version of the LNA

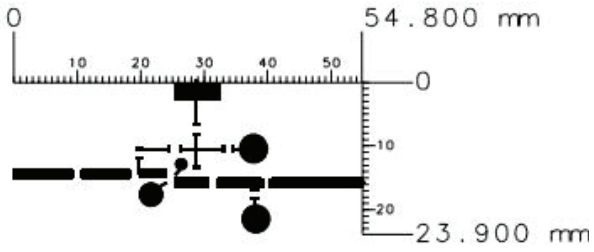

Figure 9. LNA layout used for PCB etching

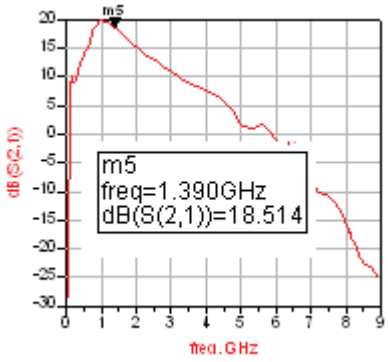

Figure 10. LNA Gain VS Frequency curve

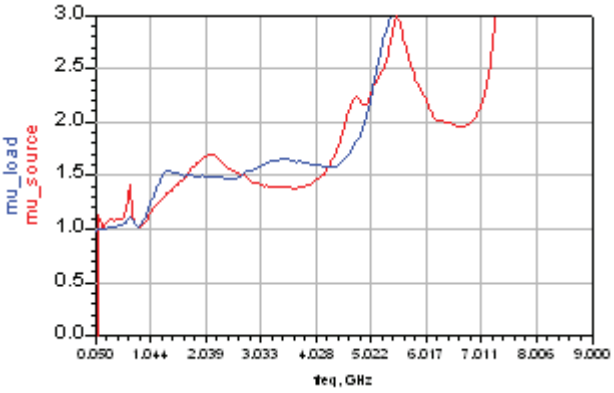

Figure 11. 'μ' stability factor

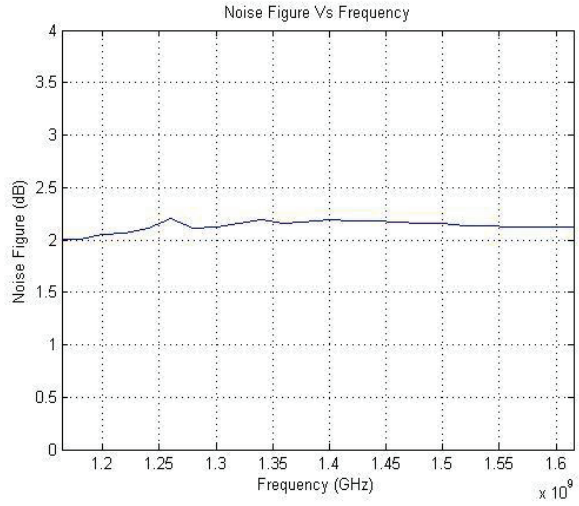

Figure 12. Plot of NF vs frequency in the entire bandwidth of the design

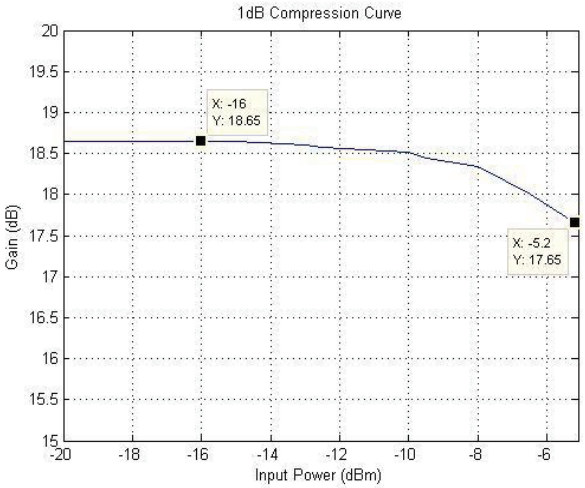

Figure 13. Input one dB compression curve. IP_{1dB} point is achieved at -5.2dBm

$|S_{21}|$. The gain of the LNA remains above the desired 18dB over the entire bandwidth. Figure 11 shows that the value of 'μ' on both the source and load impedance side is always greater than unity. Thus the LNA design is inherently stable at all frequencies. Figure 12 shows that noise figure is in the range from 2.0dB to 2.18dB over the entire bandwidth. Figure 13 shows the 1dB compression curve for the LNA. The input one dB compression point (P_{1dB}) is achieved at -5.2dBm. Therefore the output P_{1dB} can be calculated by (1).

$$P_{1dB\ output} = P_{1dB\ input}\ (dBm) + Gain\ (dB) \quad (1)$$

$$= -5.2 + 18.5 = 13.3dBm$$

A two-tone test was performed on the LNA and the results showed that when the power of the fundamental component was 0.22dBm the power of the third order intermodulation product was -46dBm. The output third order intercept point (OIP3) can be calculated from $P1dB_{\ output}$ by (2) and also from the two-tone test by (3). The value of OIP_3 obtained using both equations is the same, thus verifying the correctness of the result.

$$OIP_3 = P_{1dB\ output}\ (dBm) + 10dB = 13.3 + 10 = 23.3dBm \quad (2)$$

$$OIP_3 = \left(\frac{3}{2} * P_{input\ tones@output} - \frac{1}{2} * P_{3rd\text{-}order\ products}\right)$$

$$= (1.5*(0.22) - 0.5*(-46.0)) = 23.33dBm \quad (3)$$

TABLE 2. Final results compared with original design specifications of the LNA

Specification Name	Design Specification	Final Value
Centre frequency	1389.75MHz	1389.75MHz
Minimum bandwidth	451.5	451.5MHz
Maximum gain deviation over bandwidth	±1.5dB	±1.3dB
Small signal gain	18 – 21dB	18.5dB
Return loss (Input/Output)	<-10dB	Input = -11dB Output= -23.5dB
Noise Figure	2dB	2.18dB
Stability	0Hz to 9GHz	0Hz to 9GHz
P1dB	3dBm	13.5dBm
OIP3	13dBm	23.5dBm
Supply voltage	5V	5V
Current Consumption	20mA	18.6mA

Table 2 compares the final results with original specifications for the LNA implementation.

CONCLUSION

Design of the proposed LNA is the first step towards successful implementation of a bandpass sampling based RF front-end capable of receiving multiple GNSS frequencies. The design, simulation, implementation and test results prove that the LNA successfully satisfied requirements of wide bandwidth, high gain, high linearity and low noise figure and a solution was also found against low frequency instability. Furthermore, compared to other similar implementations, this work has a higher gain and yet has comparable noise figure, linearity and power consumption. Different methods of stabilization have been considered and their results tabulated. The implementation was perfected over a number of versions and the intermediate results of every version are also detailed. Future modifications could include addition of a linear RF filtering stage after the LNA to remove the unwanted frequency band from 1300MHz to 1559MHz. Work on such a filter has already begun at the GNSS Receiver Group of our university.

ACKNOWLEDGMENT

The research leading to these results has received funding from the European Community Seventh Framework Programme (FP7/2007-2013) under grant agreement number 227890.

REFERENCES

[1] Navstar GPS, Global Positioning System Interface Control Document, ICD-GPS-200D, 10th October, 1993

[2] Galileo Open Service, Signal in Space Interface Control Document, (OS SIS ICD, Draft 1), February 2008

[3] Global Navigation Satellite System (GLONASS), Interface Control Document, Coordination Scientific Information Center, Moscow, 2002

[4] Rodney G. Vaughan, Neil L. Scott, & D. Rod White, "The Theory of Bandpass Sampling", IEEE Transactions on Signal Processing. Vol. 39, No. 9. September 1991

[5] Dennis M. Akos, Michael Stockmaster, James B. Y. Tsui, & Joe Caschera, "Direct Bandpass Sampling of Multiple Distinct RF Signals", IEEE Transactions on Communications, Vol. 47, No. 7, July 1999

[6] Ngai Wong & Tung-Sang Ng, "An Efficient Algorithm for Downconverting Multiple Bandpass Signals Using Bandpass Sampling", IEEE International Conference on Communications Proceedings, Helsinki, Finland, June 2001, v. 3, p. 910-914

[7] Ching-Hsiang Tseng & Sun-Chung Chou, "Direct Downconversion of Multiband RF Signals Using Bandpass Sampling", IEEE Transactions on Wireless Communications, Vol. 5, No. 1, January 2006

[8] Jie-Cherng Liu, "Bandpass Sampling of Multiple Single Sideband RF Signals", ISCCSP 2008, Malta, 12-14 March 2008

[9] Mark L. Psiaki, Steven P. Powell, Hee Jung, & Paul M. Kintner, "Design and Practical Implementation of Multifrequency RF Front Ends Using Direct RF Sampling", IEEE Transactions on Microwave Theory and Techniques, Vol. 53, No. 10, October 2005

[10] S. Blaakmeer, E.A.M. Klumperink, B. Nauta, D.M.W. Leenaerts, "An Inductorless Wideband Balun-LNA in 65nm CMOS with Balanced Output", 33rd European Solid State Circuits Conference, ESSCIRC, 11-13 Sept. 2007 , München, Germany .

[11] Md. M. Hossain, "Design of RF Front End for Multi-Band Multi-System GNSS Receivers", M.Sc. Thesis, University of Gävle, January, 2008.

[12] P. Kovár, P. Kacmarík, F. Vejražka, "Universal Front End for Software GNSS Receiver", Proceedings of the 13th IAIN World Congress, Stockholm, 27-30 October 2009. Published by the Nordic Institute of Navigation

[13] Veena G Dikshit, "Development of Global Navigation Satellite System (GNSS) Receiver", DRDO-IISc Program on Mathematical Engineering Workshop, Banglore, September 2007

Available: http://pal.ece.iisc.ernet.in/PAM/work07.html

[14] Datasheet for BFP420 NPN Silicon RF Transistor, Infineon, April, 2007

[15] Reinhold Ludwig, Pavel Bretchko, RF Circuit Design – Theory and Applications, Prentice Hall 2000, ISBN 0130953237

[16] David M. Pozar, Microwave Engineering, Third Edition, Wiley 2004, ISBN 0471448788

[17] RFDude.com, RFdude.com LLC,

Available: http://tools.rfdude.com/RFdude_Smith_Chart_Program/RFdude_smith_chart_program.html